Indian Journal of Radio & Space Physics
Vol 43, June 2014, pp 235-242

FDTD based SAR analysis in human head using irregular volume averaging techniques of different resolutions at GSM 900 band

Md Faruk Ali[1,$,*] & Sudhabindu Ray[2,#]

[1]Department of Electronics and Instrumentation Engineering, Nazrul Centenary Polytechnic, Rupnarayanpur, Burdwan 713 335, India

[2]Department of Electronics and Telecommunication Engineering, Jadavpur University, Jadavpur, Kolkata 700 032, India

E-mail: [$]faruk_ali@rediffmail.com; [#]sudhabin@etce.jdvu.ac.in

Received 22 May 2013; revised 30 May 2014; accepted 04 June 2014

Specific absorption rate (SAR) induced inside human head in the near-field of a mobile phone antenna has been investigated for three different SAR resolutions using Finite Difference in Time Domain (FDTD) method at GSM 900 band. Voxel based anthropomorphic human head model, consisting of different anatomical tissues, is used to calculate the peak SAR values averaged over 10-g, 1-g and 0.1-g mass. It is observed that the maximum local SAR increases significantly for smaller mass averages.

Keywords: Specific absorption rate, Finite Difference in Time Domain (FDTD) method, Human head model

PACS Nos: 84.40.Ua; *87.50.sg*

1 Introduction

Personal wireless communication devices like cell phones or chordless phones are normally held very close to head while communicating with others. When these devices are in use, electromagnetic (EM) waves radiated from the transmitting antenna of the phone directly pass through users head and significant portion of the radiated power carrying by EM waves is absorbed by head tissues. These energy absorptions are not distributive in nature and may cause localized radio frequency (RF) energy deposition in the form of nodes and damages DNA of the living tissues[1,2]. It is also reported that prolonged EM exposure may also damage DNA structure for the digestive enzyme leaking from lysosomes[3]. Salford[4] experimentally showed that a cell with large amount of damage of DNA and its ineffective recovery may enter to an irreversible state of dormancy or may trigger cell suicide or unregulated cell division, which can lead to the formation of a cancerous tumor. It has also been reported that exposure to the EM radiation emitted from a cellular phone even lower than that of the commercially available cellular phone causes to open the blood brain barrier which can allow the release of dangerous chemicals into the brain, leak hemoglobin and can cause heart diseases and kidney stones indirectly[5,6]. Thus, the interaction of EM waves, radiated from mobile or any other wireless communication devices, with human head and other body parts causes adverse biological effects[7].

Safety guidelines or standards for protecting human head and other body parts from the adverse biological effects due to RF exposure have been issued in various countries and states, in which the basic safety limits are being set in terms of specific absorption rate (SAR). SAR is defined as the rate at which a person absorbs EM energy per unit mass tissue[8]. In theses safety guidelines or standards, a tissue volume over which the SAR should be averaged is required for safety evaluation. SAR averaged over X-g of tissue can be denoted by X-g SAR. In this way, local peak SAR averaged over 10-g and 1-g of tissue are called peak 10-g SAR and peak 1-g SAR, respectively. The tissue volume required for SAR average is still not harmonized among the different countries and states[9]. In USA, Institute of Electrical and Electronics Engineers (IEEE)[10] and Federal Communication Commission (FCC)[11] have recommended peak 1-g SAR not exceeding 1.6 W kg^{-1} as the upper safety limit. But in Europe and Japan, International Commission on non-Ionizing Radiation Protection (ICNIRP)[12] has recommended peak 10-g SAR not exceeding 2.0 W kg^{-1} as the upper safety limit.

There are two separate recommended practices developed to obtain SAR. One is based on experimental techniques and the other is based on numerical EM techniques[13]. Robot-controlled miniature field probes are used to scan the electric field inside a homogeneous tissue-simulating liquid filled anthropomorphic human body model in the experimental technique. On the other hand, in numerical technique, full wave numerical methods like Finite Difference in Time Domain (FDTD) method, Finite Element Method (FEM) or Moment Method (MoM) are used to solve Maxwell's equations in a heterogeneous representation of the human head or other body parts developed from CT or MRI scans of human head or other body parts, respectively.

In the experimental technique, the homogeneous body model is not a faithful representation of the heterogeneous human head or other body parts. On the other hand, direct measurement of SAR is not possible inside a living human head or body parts using the experimental techniques. Therefore, generally the numerical technique is used to calculate EM field components and SAR inside human head or body parts. FDTD[14] method is one of the widely used techniques to simulate the EM field distributions in three dimensional structures. Calculation of SAR and maximum local SAR (MLSAR) in human head is reported in several research papers and articles[15-21].

In this work, variations of peak SAR with frequency and distance have been studied for different averaging mass resolutions using FDTD method for a realistic grounded human head model consisting of twenty two types of tissues exposed to EM waves radiated from a mobile phone antenna designed for GSM 900 band (890-960 MHZ). For all simulations, the antenna is placed in the close vicinity of the head model. Simulated SAR values are compared with the available safety limits. RF radiation safety standards are normally set in terms of 10-g and 1-g SAR in different countries and these two mass averaging resolutions are included in this study. Resolution of 0.1-g SAR is also included in this study, where safety standards are not available. In-house FDTD code is developed using commercially available MATLAB[22] software to carry out EM simulations. Finite Integration Technique (FIT) based commercially available EM simulation software CST Microwave Studio®[23] is used to validate the performance of the in-house FDTD code.

2 Model and Method for analysis

2.1 Human head model

The human head model has been constructed from Zubal phantom[24], which is based on CT scan data of a 35 year old male weighing 155 lbs and measuring 5′10″ in height. Mid-saggital and mid-coronal geometrical view of the Zubal phantom are shown in Fig. 1 (a and b). The man has been considered to be clinically normal and had no head abnormalities. MATLAB program is used to read, resample and reshape the phantom volume data consisting of 128×128×243 cubic cells. To simplify the numerical calculations, resolution of volume is reduced by 50% and other parts of the human body, except the head, are excluded in the simulation.

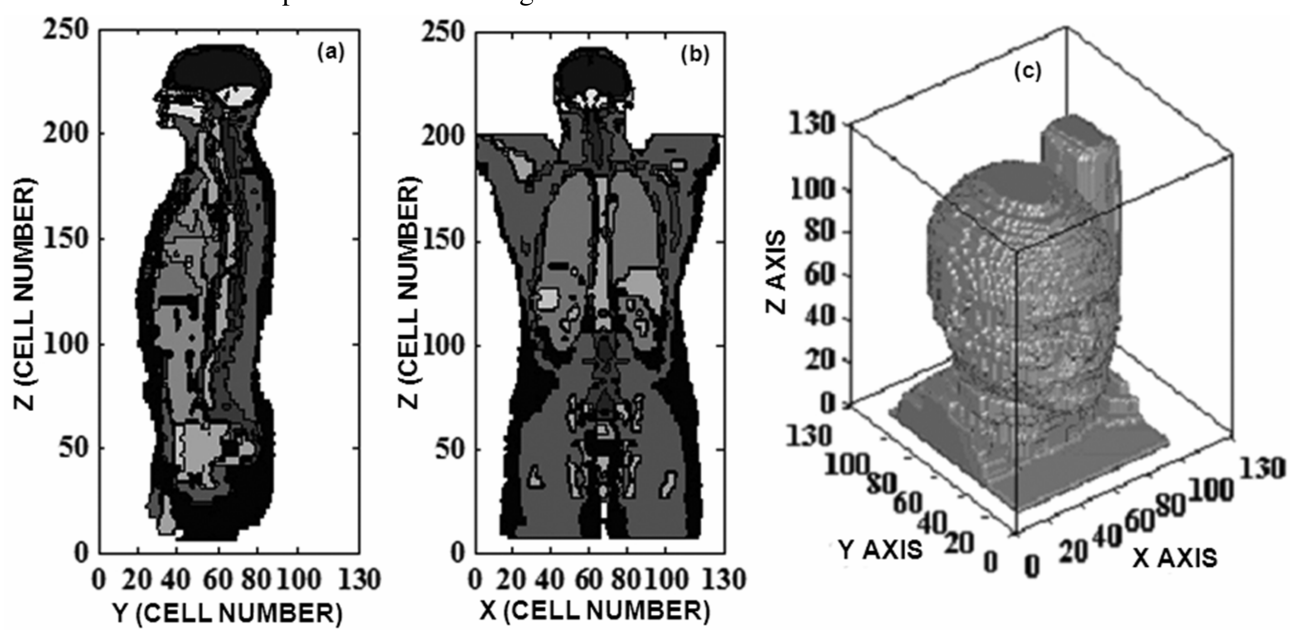

Fig. 1 — (a) Mid-saggital; (b) mid-coronal; and (c) 3-dimensional geometrical view of human head model along with mobile handset

Due to huge complexity of the human head, limitations of FDTD method and computational resources, several assumptions have been made in calculations of SAR. In this work SAR has been calculated considering only twenty two types of head tissues but it is actually consisting of several types of tissue of varying dielectric properties. Except head, other parts of human body have been excluded in the simulation and the hand-held cellular phone is modeled as an equivalent mobile phone antenna. The 3-dimensional geometry of the human head model along with the mobile handset used in the simulation is shown in Fig. 1 (c). The head is comprised of twenty two types of tissues; i.e. brain, cerebellum, skin, bone, muscle, fat, lens, eyeball, tongue, blood, cartilage, cerebral falx, parotid gland, retina, teeth, trachea, spinal chord, nerve, eye sclera, bone marrow, pituitary gland and mouth cavity/sinuses. Mass density (ρ), mass of one cell, relative dielectric constant (ε_r) and conductivity (σ) of different tissues are obtained from the literature[25]. Frequency dependent, ε_r and σ, are determined by interpolating the available data.

2.2 Ground plane

In reality, head is connected to a lossy dielectric body mass placed on real ground. But the head exposure in the near field of the antenna is highly localized and the conductive plane might influence the absorption of energy. Moreover, considering a ground plane in close contact with the head model seems far from a realistic hypothesis. But in this work, as to simplify the numerical calculations other parts of the human body, except the head, are excluded. Human head floating in free space is not a realistic situation. So, in order to approach towards a practical condition, a conductive ground plane is added under the human head model which is in contact with the perfectly matched layer forming an energy sink.

2.3 FDTD method

In the present study, FDTD method has been used to investigate the interactions between the human head model and EM waves radiated from a mobile phone antenna[26]. To ensure the stability of the FDTD analysis, time step (Δt) must be limited by the following Courant stability criterion[27]:

$$\Delta t \le \frac{\left(\frac{1}{\Delta_x^{\,2}}+\frac{1}{\Delta_y^{\,2}}+\frac{1}{\Delta_z^{\,2}}\right)^{-1/2}}{c} \qquad \ldots (1)$$

where, c, is the speed of light in free space; and Δ_x, Δ_y and Δ_z, the spatial increment along x, y and z-axis, respectively. If the time step (Δt) does not satisfy Eq. (1), then the simulation will not be stable. In an unstable condition, the computed *E* and *H* field components will increase without limit as the simulation progress. Number of steps (*NSTEPS*) the FDTD program iterated is obtained by the relation[28]:

$$NSTEPS = n \cdot \frac{1}{f\,\Delta t} \qquad \ldots (2)$$

where, *f.* is the frequency; and *n,* number of period of oscillations or time cycles required for the internal *E* fields to reach the steady state condition or the input pulse has died out.

In this study, the simulation domain enclosing head model, mobile phone and Absorbing Boundary Condition (ABC) consists of 65×74×70 Yee cells with cell dimension of 4 mm × 4 mm × 5 mm and $\Delta t = 8.21\times10^{-12}$ s. At 925 MHz, only about three time cycles have been found to be sufficient to reach the steady state condition. Therefore, value of *NSTEPS* obtained from the Eq. (2) is 360.

2.4 Perfectly Matched Layer (PML)

Perfectly Matched Layer (PML) has been used as ABC to remove unwanted reflection from the boundary. When electromagnetic wave enters into the PML, it decays successively with space and its effects get nullified at the boundary layer. In this simulation 5Δ Unsplit Step 3D- PML has been used[29]. The PML is spaced 2Δ cells from the closest surface of the source mobile phone handset and scatterer head model.

2.5 Antenna model

A compact dual-band Planar Inverted Folded Antenna (PIFA) used in GSM mobile phone is applied in this study as an EM source. The 3-dimensional geometry of the PIFA shown in Fig. 2 (a) has been imported from CAD file. The PIFA is encapsulated within a mobile handset housing the dimension 72 mm × 169 mm × 20 mm as shown in the Fig. 2 (b).

In real case, for normal use value of radiated power from cellular phone is 250 mW but it can reach to 1 W or 2 W, when the phone is far away from the mobile base station[30]. In this study, the PIFA is fed with 0.6 W power and placed in closed vicinity of the human head model. Frequency dependent reflection coefficient $S_{11}(f)$ of the PIFA is determined from the ratio of the Discrete Fourier Transform (DFT) of incident and reflected waveforms[17]:

$$S_{11}(f) = \frac{DFT\left[E_{ref}\right]}{DFT\left[E_{inc}\right]} \quad \ldots (3)$$

where, E_{inc}, *is* incident electric field; and E_{ref}, reflected electric field.

S_{11} is computed in dB by:

$$S_{11} = 20\log_{10}\left(\left|S_{11}\right|\right) \quad \ldots (4)$$

2.6 SAR calculation

From the converged solutions the local SAR at (*i,j,k*)th cell inside the head is obtained from the following relation[20]:

$$\mathrm{SAR}(i,j,k) = \frac{\sigma(i,j,k)\left|\hat{E}(i,j,k)\right|^2}{2\rho(i,j,k)} = \frac{\sigma(i,j,k)\left\{\left|\hat{E}_x(i,j,k)\right|^2 + \left|\hat{E}_y(i,j,k)\right|^2 + \left|\hat{E}_z(i,j,k)\right|^2\right\}}{2\rho(i,j,k)} \quad (\mathrm{W\ kg^{-1}}) \quad \ldots (5)$$

where, $\hat{E}_x$, $\hat{E}_y$ and $\hat{E}_z$, are the peak values of the electric-field components (V m^{-1}); σ, conductivity (S m^{-1}); and ρ, mass density of the head tissues (kg m^{-3}).

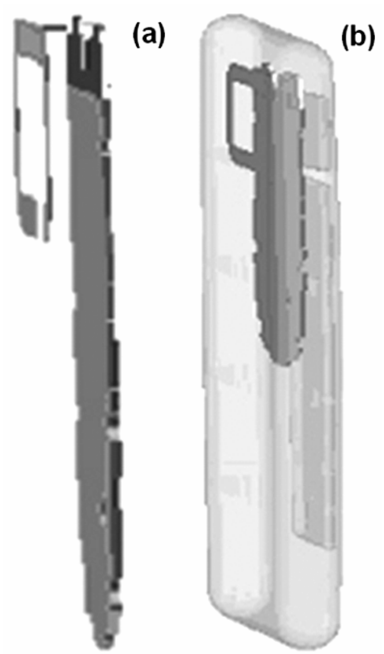

Fig. 2 — (a) PIFA; and (b) PIFA encapsulated in the mobile handset housing

Considerations on the irregular volume averaging, peak 10-g, 1-g and 0.1-g SAR has been obtained in this study[31]. In the irregular volume averaging technique, peak 10-g SAR is obtained by the following procedure. First of all, maximum value of local SAR in an FDTD cell is calculated. Then the neighbour FDTD cell with maximum value of local SAR is searched and clubbed with the earlier cell, and so on. The process is repeated until total mass of the FDTD cells becomes equal to the required mass of 10 g. Similarly peak 1-g and 0.1-g SAR are calculated.

3 Results and Discussion

Return loss of the mobile phone antenna (PIFA) is computed using the MATLAB program and compared with CST Microwave Studio® results. Variations of S_{11} with frequency for the mobile phone antenna computed using MATLAB and CST Microwave Studio® are shown in Fig. 3. The result obtained using the MATLAB program shows close agreement with that obtained from CST Microwave Studio®. At the fundamental mode, the antenna resonates at 925 MHz and the value of S_{11} remains below –10 dB within GSM 900 band. Values of S_{11} at the fundamental resonance frequency obtained from MATLAB program and CST Microwave Studio® are –22.21 dB and –24.95 dB, respectively.

After return loss calculation is over, head model along with the antenna is simulated for 0.7 to 1.3 GHz. SAR distributions at the mid-sagittal YZ, mid-coronal XZ and transverse XY planes in dB scale at 925 MHz are shown in the Fig. 4 (a-c). The distribution of SAR inside the head for all sectional

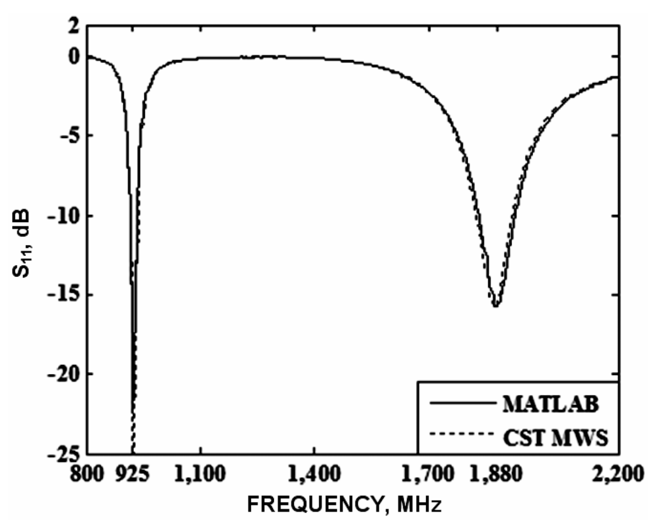

Fig. 3 — Variation of S_{11} *vs* frequency of the mobile phone antenna (PIFA) in free space

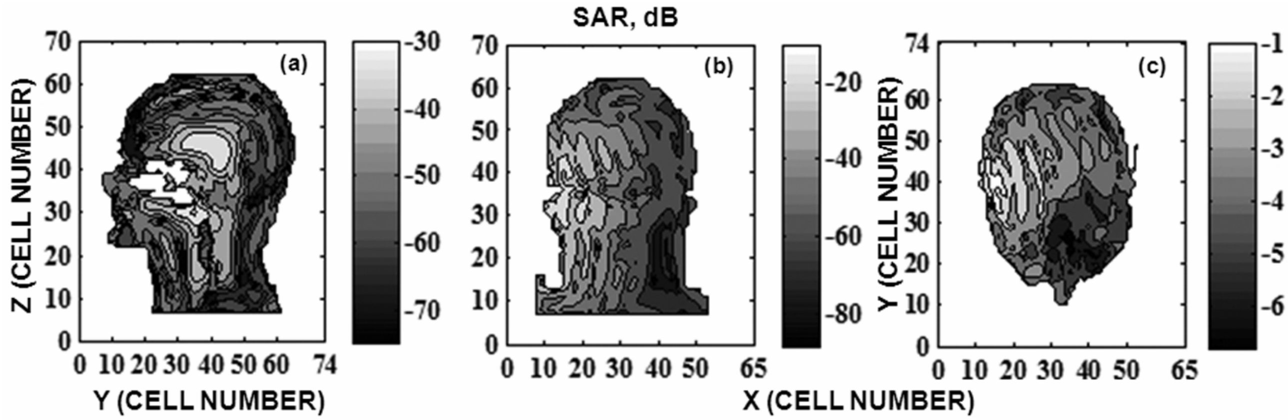

Fig. 4 — SAR distribution in: (a) mid-sagittal YZ plane (X = 34 Yee cell); (b) mid-coronal XZ plane (Y = 37 Yee cell); and (c) transverse XY plane (Z = 40 Yee cell) of the human head model

Table 1 — Maximum value of peak gram average SARs induced in the human head tissues at 925 MHz

Tissue Type	Maximum peak 0.1-g SAR	Maximum peak 1-g SAR	Maximum peak 10-g SAR
Brain	0.5620	0.2555	0.1342
Cerebellum	0.0492	0.0333	0.0164
Skin	3.7629	2.7649	0.8951
Bone	0.0471	0.0490	0.0291
Muscle	2.3434	1.5917	0.7448
Fat	0.3419	0.1922	0.0310
Lense	2.6203e-004	1.6395e-004	8.2176e-005
Eye	0.0033	0.0027	9.0376e-004
Tongue	0.0262	0.0168	0.0038
Blood	0.4633	0.3374	0.1001
Cartilage	2.5529	1.2733	0.4048
Cerebral falx	0.0149	0.0047	9.2749e-004
Esophagus	8.3832e-004	3.2804e-004	1.0390e-004
Pons	0.0194	0.0149	0.0064
Teeth	5.4255e-004	3.2381e-004	8.5599e-005
Trachea	0.0026	0.0013	4.4126e-004
Spinal chord	0.0017	0.0014	8.4875e-004
Nerve	0.0028	0.0015	3.4515e-004
Dens of axis	0.0049	0.0032	0.0026
Bone marrow	1.9832e-004	1.4191e-004	5.3735e-005
Thyroid	7.5321e-004	5.0310e-004	3.5714e-004
Mouth cavity/ sinuses	0.0000	0.0000	0.0000

planes shows similarity with propagating wave field pattern. In mid-sagittal plane, SAR holds higher value in the central parts and the average level decays gradually towards outer region. In mid-coronal plane, SAR is found maximum near the outer region of head close to antenna and then decreases and increases periodically with continuous decrease in the average level with the increases of distance from antenna. In transverse plane, SAR is found maximum in the vicinity of right ear close to antenna and then decreases periodically with increase of distance from antenna.

Maximum value of peak 10-g, 1-g and 0.1-g SARs obtained at 925 MHz in different type of head tissues are listed in Table 1. From the table, it is seen that maximum value of peak gram averaged SARs for all resolutions are obtained in skin tissue. Whereas, minimum value of peak gram averaged SARs for all resolutions are obtained in bone marrow tissues. Mouth or sinuses cavities are filled with air and therefore, have zero conductivity so no SAR is induced in it. Calculation of peak 0.1-g SAR within the bone and teeth tissues is not possible using the irregular volume averaging technique because the mass of one cell for these tissues is 0.148 g which is greater than 0.1 g. Using the cube averaging technique, peak 0.1-g SAR is calculated within the bone and teeth tissues where mass of one cell is not been considered. Peak 0.1-g SAR is obtained by averaging over cube of 0.1 g masses made of bone/teeth tissues. Corresponding SAR values obtained are 0.0471 and 5.4255×10^{-4} W kg^{-1}, respectively.

Variation of peak SAR with distance for 10-g, 1-g and 0.1-g mass in saggital and coronal planes at 925 MHz are shown in Fig. 5 (a and b), where, D_x and D_y, are the measured distances along x and y-axis, respectively. In saggital plane for all resolutions, peak SAR value attains maximum near the position of the antenna and decreases exponentially with either increase or decrease of D_y. But in coronal plane for all resolutions, peak SAR value attains maximum in the

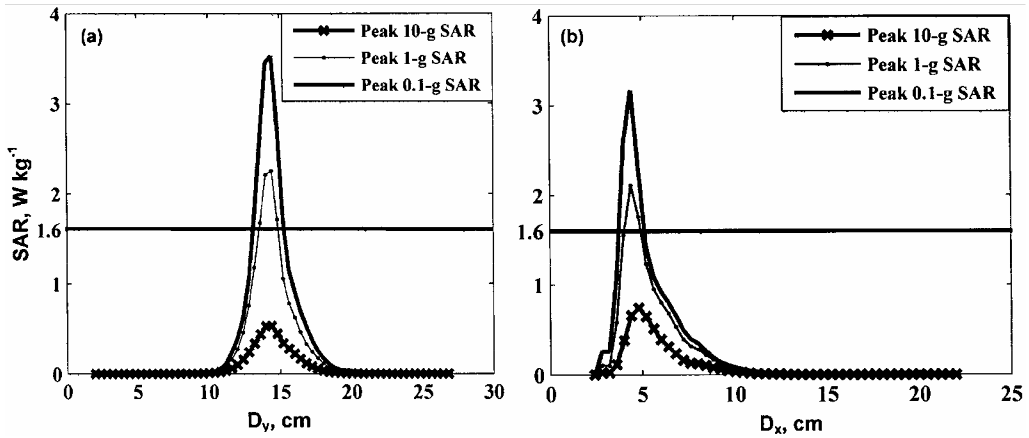

Fig. 5 — Peak 10-g, 1-g and 0.1-g SAR *vs* distance in the (a) sagital; and (b) coronal planes of the human head model at 925 MHz for $d = 0.4$ cm

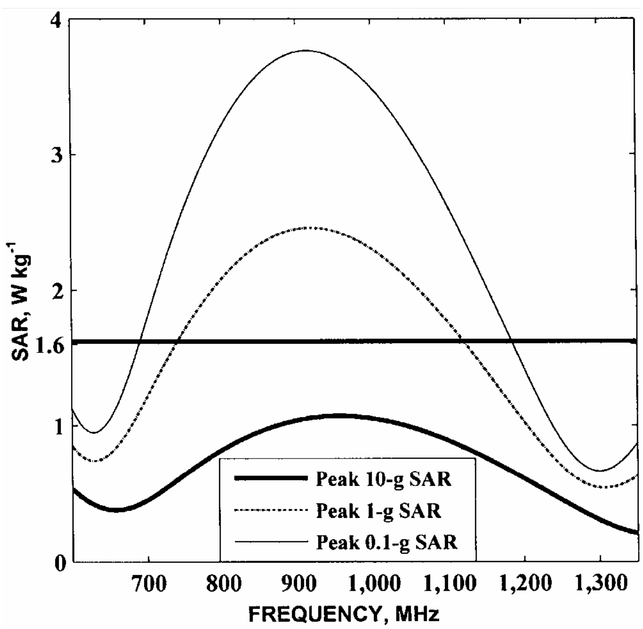

Fig. 6 — Peak 10-g, 1-g and 0.1-g SAR *vs* frequency induced in the realistic grounded human head model for d = 4 mm

position close to the antenna and decreases exponentially with increase of D_x. The maximum value of peak 10-g, 1-g and 0.1-g SARs obtained in the saggital plane are 0.53, 2.26 and 3.53 W kg^{-1}, respectively and that obtained in the coronal plane are 0.74, 2.11 and 3.18 W kg^{-1}, respectively. In the both planes, value of peak 10-g SAR is below the recommended safety limit of 2.0 W kg^{-1}, whereas the value of peak 1-g SAR is more than the recommended safety limit of 1.6 W kg^{-1}.

Variation of peak SAR with frequency in the range of 700 MHz to 1.3 GHz for 10-g, 1-g and 0.1-g mass is shown in Fig. 6. For all resolutions, peak SAR value initially increases with increase of frequency and attains maximum near the antenna resonance frequency then decreases with further increase of frequency. Because at the antenna resonance frequency, maximum power is transmitted from the antenna to head model due to good impedance matching. The maximum value of peak 10-g, 1-g and 0.1-g SARs induced in the head are 1.07, 2.45 and 3.75 W kg^{-1}, respectively. These result shows that the absorbed power at the frequency band of study is not uniform throughout the 10-g or 1-g mass of the head tissues. The absorbed power at any frequency within the band of study is concentrated to smaller mass in the form of node.

It is seen that maximum value of peak 10-g, 1-g and 0.1-g SARs induced in the head model obtained by variation of peak SAR with frequency analysis are higher than that obtained in saggital and coronal planes at 925 MHz. This unwanted mismatch occurs due to inhomogeneous nature of realistic human head model and the averaging schemes. In case of saggital and coronal plane analysis, peak gram average SARs are obtained by finding the value of maximum local SAR in 2-D but in the case of variation of peak SAR with frequency analysis, peak gram average SARs are obtained by finding the value of maximum local SAR in 3-D.

4 Conclusions

In the present work, SAR distributions and peak SAR averaged over 10-g, 1-g and 0.1-g mass of human head tissue induced inside a CT scan data based head model consisting of twenty two types of tissues have been studied using FDTD method considering the electrical properties of different tissues for GSM 900 band. To find accurate local maximum SAR, irregular volume averaging technique is used for different mass averages except for the calculation of 0.1-g SAR in bone and teeth tissues, where it is calculated using cube averaging technique. Variation of peak 10-g, 1-g and 0.1-g SARs with frequencies and distances without considering the multiplexing or modulation techniques used for mobile communication systems. Variation of peak 10-g, 1-g and 0.1-g SARs with frequency in the range 700 MHZ - 1.3 GHz shows that peak SAR values attain to maxima near the antenna resonance frequency. Variation of peak 10-g, 1-g and 0.1-g SARs with distance at 925 MHz in saggital and coronal planes show that for smaller mass average, the peak SAR value increases significantly and the value of peak 0.1-g SAR has been found more than three times of peak 10-g SAR. Maximum values of 10-g, 1-g and 0.1-g SARs induced in the head model are 1.07, 2.45 g and 3.75 W kg^{-1}, respectively for 0.6 W applied power to the mobile phone antenna. It is observed that 0.1-g SAR provides more detail information regarding variation of energy absorption inside body and more suitable for tissues with very small volumes and masses with compared to 10-g or 1-g SARs.

Acknowledgement

The authors are thankful to Dr George Zubal, Department of Diagnostic Radiology, Yale School of Medicine, New Haven for technical assistance.

References

1 Philips J L, Ivaschuk O, Ishida-Jones T, Jones R A, Campbell-Beachler M & Haggren, W, DNA damage in Molt-4 T-lymphoblastoid cells exposed to cellular telephone radiofrequency fields in vitro, *Bioelectrochem Bioenergetics (Switzerland)*, 45 (1998) pp 103-110, doi: 10.1016/S0302-4598(98)00074-9.

2 Mashevich M, Exposure of human peripheral blood lymphocytes to electromagnetic fields associated with cellular phones leads to chromosomal instability, *Bioelectromagnetics (USA)*, 24 (2003) 82.

3 Goldsworthy Andrew*, The Dangers of Electromagnetic Smog*, Aug 2007, http://www.hese-project.org/hese-uk/en/papers/electrosmog_dangers.pdf.

4 Salford L, Experimental studies of brain tumor development during exposure to continuous and pulsed 915 MHz radio frequency radiation, *Bioelectrochem Bioenergetics (Switzerland)*, 30 (1993) pp 313-318.

5 Microwaves open up Blood Brain Barrier, Svenska Dagbladet (Sweden), 15 Sep 1999, http://www.oocities.org/uk_nirvana/brainblood.htm.

6 Harish, Sarah, Now Mobiles Give You Kidney Damage, *Daily Mail*, 13 Dec 1999, EPI1812.

7 Kumar V, Vats R P, Goyal S, Kumar S & Pathak P P, Interaction of electromagnetic radiation with human body, *Indian J Radio Space Phys*, 37 (2008) pp 131-134.

8 Shabani H, Md Islam R, Alam AHM Z & Abd EI-Raouf H E, EM Radiation from Wi-LAN base station and its' effects in human body, 5th *International Conference on Electrical and Computer Engineering* (*ICECE 2008*), (IEEE, USA), 2008, pp 86-91.

9 Wang J & Fujiwara O, *Dosimetry in the human head for portable telephones*, http://rp.iszf.irk.ru/hawk/ URSI2002/ rsreview/3.pdf.

10 American National Standard, Safety levels with respect to exposure to radio frequency electromagnetic fields, 3 kHz to 300 GHz, *ANSI/ (*IEEE C95.1), (ANSI, Washington), 1992.

11 United States Federal Communications Commission (US FCC) safety guidelines, *Radio Frequency safety* (Office of Engineering and Technology (OET)), http://www.fcc.gov/oet/rfsafety/rf-faqs.html.

12 International Commission on non-Ionizing Radiation Protection, ICNIRP statement-Health issues related to the use of hand –held radiotelephones and base transmitters, *Health Phys (USA)*, 70 (4) (1996) pp 587-593.

13 Osepchuk J M & Petersen R C, Safety Standards for Exposure to RF Electromagnetic Fields, *IEEE Microw Mag (USA)*, 2 (2001) pp 55-69.

14 Yee K S, Numerical solution of initial boundary value problems involving Maxwell's equations of isotropic media, *IEEE Trans Antenna Propag (USA)*, 14 (1966) pp 302-307.

15 Choi D G, Shin C S, Kim N K & Shin H S, Design and SAR analysis of Broadband PIFA with triple band, *Progress in Electromagnetics Research Symposium*, Hangzhur, China (The Electromagnetics Academy, Cambridge, MA), 2005 pp 22–26.

16 Ali M F & Ray S, SAR Analysis on human head exposed to radiating dipole antenna for 500 MHz – 5 GHz frequency band using FDTD method, *National Conference on Communications*, IIT Bombay, India, (Allied Publishers, New Delhi, India), 2008, pp 481-485.

17 Ali M F & Ray S, SAR Analysis in a spherical inhomogeneous human head model exposed to radiating dipole antenna for 500 MHz – 3 GHz Using FDTD method, *Int J Microw Opt Technol (USA)*, 4 (2009) pp35-40.

18 Homsup N & Homsup W, FDTD simulation of a mobile phone operating near a metal wall, *J Computers* (*UK*), 4 (2009) pp 168-175.

19 Ali M F & Ray S, SAR analysis for handheld mobile phone using DICOM based Voxel model, *J Microw, Optoelectron Electromagn Appl (Brazil)*, 12 (2013) AoP126b-AoP138b.

20 Gandhi O P, Gianluca Lazzi & Cynthia Furse M, Electromagnetic absorption in the human head and neck for mobile telephones at 835 and 1900 MHz, *IEEE Trans Microw Theory Tech* (*USA*), 44 (1996) pp 1884-1897.

21 Hirata A, Morita M & Shiozawa T, Temperature increase in the human head due to a dipole antenna at microwave frequencies, *IEEE Trans Electromagn Compat* (*USA*), 45 (2003) pp 109-116.

22 MATLAB® R2008b, *The Language of Technical Computing software for engineers and scientists* (The MathWorks), http://www.mathworks.in/index.html?s_cid=pl_homepage.

23 CST Microwave Studio Suite, *3D Electromagnetic Simulation Software*, 2010, http://www.cst.com.

24 The Zubal Phantom data, *MRI Head Phantom Data Description*,http://noodle.med.yale.edu/phantom/getzubdesc.htm.

25 *Dielectric properties of the human body tissue in the frequency range of 10 Hz - 100GHz,* http://niremf.ifac.cnr.it/tissprop.

26 Sullivan D M, *Electromagnetic simulation using the FDTD Method* (*IEEE Press*, New York, USA), 2000.

27 Taflove A, Computation electrodynamics: *The Finite-Difference Time Domain Method* (Artech House, Boston, United States), 1995.

28 Sullivan D M, Broup D T & Gandhi O P, Use of the Finite-Difference Time-Domain Method in calculating EM absorption in human tissues, *IEEE Trans Biomed Eng* (*USA*), 34 (1987) 148-158.

29 Sullivan D M, An unsplit Step 3-D PML for use with the FDTD method, *IEEE Microw Guid Wave Lett* (*USA*), 7 (1997) pp 184-186.

30 Islam M T & Faruque M R I, Reduction of specific absorption rate (SAR) in the human head with ferrite material and metamaterial, *Prog Electromagn Res C* (*Hong Kong)*, 9 (2009) pp 47-58.

31 Watanabe S & Martens L, Comparison of averaging procedures for SAR distributions at 900 and 1800 MHz, *IEEE Trans Microw Theory Tech (USA)*, 48 (2000) pp 2180-2184.